Journal of Inflammation Research

Dovepress
open access to scientific and medical research

Open Access Full Text Article

ORIGINAL RESEARCH

Lung-Gut Microbiota and Tryptophan Metabolites Changes in Neonatal Acute Respiratory Distress Syndrome

Jingli Yang[1–4], Yu He[1–5], Qing Ai[1–4], Chan Liu[1–4], Qiqi Ruan[1–4], Yuan Shi[1–4]

[1]Department of Neonatology, Children's Hospital of Chongqing Medical University, Chongqing, People's Republic of China; [2]National Clinical Research Center for Child Health and Disorders, Chongqing, People's Republic of China; [3]Ministry of Education Key Laboratory of Child Development and Disorders, Children's Hospital of Chongqing Medical University, Chongqing, People's Republic of China; [4]Chongqing Key Laboratory of Child Infection and Immunity, Children's Hospital of Chongqing Medical University, Chongqing, People's Republic of China; [5]Department of Neonatology, Jiangxi Hospital Affiliated to Children's Hospital of Chongqing Medical University, Jiangxi, People's Republic of China

Correspondence: Yuan Shi, Department of Neonatology, Children's Hospital of Chongqing Medical University, Chongqing, 400014, People's Republic of China, Email shiyuan@hospital.cqmu.edu.cn

Purpose: Neonatal Acute Respiratory Distress Syndrome (NARDS) is a severe respiratory crisis threatening neonatal life. We aim to identify changes in the lung-gut microbiota and lung-plasma tryptophan metabolites in NARDS neonates to provide a differentiated tool and aid in finding potential therapeutic targets.

Patients and Methods: Lower respiratory secretions, faeces and plasma were collected from 50 neonates including 25 NARDS patients (10 patients with mild NARDS in the NARDS_M group and 15 patients with moderate-to-severe NARDS in the NARDS_S group) and 25 control patients screened based on gestational age, postnatal age and birth weight. Lower airway secretions and feces underwent 16S rRNA gene sequencing to understand the microbial communities in the lung and gut, while lower airway secretions and plasma underwent LC-MS analysis to understand tryptophan metabolites in the lung and blood. Correlation analyses were performed by comparing differences in microbiota and tryptophan metabolites between NARDS and control, NARDS_S and NARDS_M groups.

Results: Significant changes in lung and gut microbiota as well as lung and plasma tryptophan metabolites were observed in NARDS neonates compared to controls. *Proteobacteria* and *Bacteroidota* were increased in the lungs of NARDS neonates, whereas *Firmicutes, Streptococcus*, and *Rothia* were reduced. *Lactobacillus* in the lungs decreased in NARDS_S neonates. Indole-3-carboxaldehyde decreased in the lungs of NARDS neonates, whereas levels of 3-hydroxykynurenine, indoleacetic acid, indolelactic acid, 3-indole propionic acid, indoxyl sulfate, kynurenine, and tryptophan decreased in the lungs of the NARDS_S neonates. Altered microbiota was significantly related to tryptophan metabolites, with changes in lung microbiota and tryptophan metabolites having better differentiated ability for NARDS diagnosis and grading compared to gut and plasma.

Conclusion: Significant changes occurred in the lung-gut microbiota and lung-plasma tryptophan metabolites of NARDS neonates. Alterations in lung microbiota and tryptophan metabolites were better discriminatory for the diagnosis and grading of NARDS.

Keywords: Neonatal acute respiratory distress syndrome, NARDS, lung microbiota, gut microbiota, tryptophan metabolites, correlation analysis, predictive diagnosis

Introduction

Neonatal Acute Respiratory Distress Syndrome (NARDS) is a severe life-threatening respiratory crisis in newborns, clinically characterized by hypoxemia, diffuse decrease in lung transmittance, and inflammatory exudation with decreased lung compliance. The etiology of NARDS is complex and can be divided into direct lung injury (such as severe pulmonary infections, pulmonary hemorrhage, meconium or amniotic fluid aspiration) and indirect lung injury (such as sepsis, necrotizing enterocolitis, asphyxia).[1] Recent multicenter cohort studies have shown mortality rates of up to 17%–24% for NARDS, making it a leading cause of neonatal mortality and disability.[2] Despite its significance, NARDS etiology and pathogenesis remain poorly understood, and effective identification tools and treatments are

Received: 13 January 2024
Accepted: 2 May 2024
Published: 15 May 2024

notably lacking. Therefore, understanding the mechanisms underlying NARDS and finding a better differentiated tool and therapeutic targets are critical.

Microbial colonies, often referred to as the "endocrine organ" of the human body, are integral players in coordinating microbial signals and immune responses for maintaining homeostasis.[3–5] Recent reports challenge the belief that lungs are sterile, revealing microbial colonies with concentrations from 10^3 to 10^5 per gram of tissue, dominated by genera such as *Prevotella, Streptococcus, Veillonella, Fusobacterium, and Haemophilus*. These colonies are closely associated with respiratory diseases.[6–9] Lung injury can alter the structure of lung microbial colonies, escalating inflammation, disrupting defenses, and triggering a feedback loop that worsens acute lung injury.[10–12] The gut, as the largest microbial reservoir, influences lung diseases through the "gut-lung axis".[13] Newborns exhibit distinct microbial community structures influenced by factors like gestational age and delivery method compared to children and adults.[14] Therefore, studying the role of the neonatal lung-gut microbiota in NARDS progression is crucial.

Microbial metabolites are a key component of the interaction between the microbiome and the host, linked to various inflammatory and metabolic diseases.[15–17] Tryptophan is a diet-derived essential amino acid that is absorbed in the gut and metabolized by microbes into indoles and derivatives such as indoleacetic acid (ILA), 3-indole propionic acid (IPA), indole-3-carboxaldehyde (ICA), and kynurenine (KYN).[5,18] After binding to the widely expressed aryl hydrocarbon receptor (AhR) and pregnane X receptor (PXR) in the barrier and immune systems, these tryptophan metabolites exhibit extensive antioxidative activity, inhibit excessive inflammation, and influence the progression of various diseases, including gastrointestinal, respiratory, neurological, and metabolic diseases, and cancers.[19–23] According to recent studies, AhR is highly active in lung endothelial cells and is a crucial player in lung barrier immunity and the immune response in respiratory diseases.[24] Currently, there have been no reports on the microbiota composition and tryptophan metabolites in newborns with NARDS. Therefore, exploring the changes in microbial structure and tryptophan metabolites in NARDS is of significant importance.

We will explore the microbial colony structure and composition of tryptophan metabolites in the lungs and intestines of NARDS neonates using a combined microbiome and metabolomics approach, and analyze the correlation between microbial communities and tryptophan metabolites. This will help us to understand the etiology and pathogenesis of NARDS, provide a better differentiated tool and find potential therapeutic targets.

Materials and Methods

Ethics and Informed Consent

This study was approved by the Ethics Review Committee of the Children's Hospital of Chongqing Medical University (Approval No. 2022-414), and written informed consent was obtained from the parents for sample collection. The feces, venous blood, and lower respiratory tract secretions were the residual samples after the corresponding clinical laboratory testing. Our study adhered to the tenets of the Declaration of Helsinki.

Participant Recruitment and Sample Collection

From October 2022 to August 2023, we evaluated patients with NARDS in the neonatal intensive care unit (NICU) of the Affiliated Children's Hospital of Chongqing Medical University using standardized criteria. The inclusion criteria were as follows: Preterm or term infants diagnosed with NARDS within one week after birth according to the 2017 "Montreux criteria", with consent of the guardian, complete clinical data and samples, these patients will be included in the NARDS group. The "Montreux criteria" for NARDS are as follows: 1) Acute onset (within 1 week). 2) Presence of diffuse, irregular opacities, infiltrates, or white-out of both lungs, not explained by other causes such as local effusions, atelectasis, Neonatal respiratory distress syndrome (NRDS), Transient tachypnea of the newborn (TTN), or congenital anomalies. 3) Pulmonary edema not explained by congenital heart disease. 4) Severity of NARDS was categorized based on the oxygenation index (OI) into mild, moderate, and severe (4–7.9 for mild, 8–15.9 for moderate, ≥16 for severe).[25] In our study, newborns diagnosed with mild NARDS were included in the NARDS_M group, while those diagnosed with moderate to severe NARDS were included in the NARDS_S group.

NARDS can occur in both premature and full-term infants, with 94% diagnosed within the first 3 days, and the acute "waterfall" inflammatory cascade is key to NARDS progression.[2,25,26] In addition, NARDS often coexists with other perinatal diseases. 40.7% of premature infants may have concomitant NRDS in the early postnatal period, while cesarean-delivered full-term infants or late preterm infants typically present with TTN, and some infants may even present with both NRDS and TTN simultaneously.[2,26,27] Furthermore, factors such as gestational age, postnatal age, and birth environment can lead to changes in the early microbial structure of newborns.[28] Therefore, selecting appropriate controls is crucial for studying the specific microbial communities and metabolites in NARDS neonates. NRDS and TTN are common pulmonary diseases in the early postnatal period, usually not complicated by pulmonary or systemic infections that significantly affect microbial structure. The postnatal age and gestational age of the NRDS and TTN patients are similar to those of NARDS patients. Therefore, selecting newborns with NRDS and TTN as controls is the most appropriate choice.

Inclusion criteria for the control group: 1) Newborns diagnosed with NRDS or TTN according to definition. NRDS is characterized by bilateral widespread collapse of alveoli and reduced exudation due to insufficient pulmonary surfactant caused by lung immaturity in newborns, presenting as progressive respiratory distress within 24 hours after birth.[29] TTN is transient respiratory distress in newborns after birth due to impaired absorption of lung fluid, typically resolving within 72 hours.[30] 2) Normal infection indicators and normal or mildly abnormal chest X-ray. 3) The control group newborns were selected based on postnatal age (±2 days), gestational age (±1 week), and birth weight (±500 grams) of the NARDS group newborns. 4) Consent of the guardian and complete clinical data and samples.

Exclusion criteria included congenital malformations affecting respiratory function, other diseases affecting microbial flora (gastrointestinal diseases such as necrotizing enterocolitis, food protein-induced enterocolitis), unavailability of clinical data and samples, and withdrawal upon request by guardians.

Newborns meeting the inclusion criteria were sampled within 24 hours of diagnosis, with collection of plasma, feces, and lower respiratory tract secretions. One milliliter of venous blood was collected in sterile anticoagulant tubes, centrifuged (4°C, 3000 rpm, 10 minutes) to obtain 300 μL of upper plasma layer. Two milliliters of lower respiratory tract secretions were collected using sterile centrifuge tubes. For infants on mechanical ventilation, lower respiratory tract secretions are aspirated by inserting a sterile suction catheter deep into the trachea. Non-intubated patients have secretions collected by inserting a sterile suction catheter below the vocal cords observed with a laryngoscope. Three grams of fresh feces were collected from the middle portion without contacting the skin or diaper. The lower respiratory tract secretion and fecal samples underwent 16S rRNA gene sequencing analysis, while the lower respiratory tract secretion and plasma samples underwent analysis of tryptophan metabolites. All samples were immediately stored at −80°C before use.

16S rRNA Gene Sequencing Analysis

DNA extraction from the frozen lower airway secretions and fecal samples by using the MagAttract PowerSoil Pro DNA Kit (Qiagen, Germany) and PF Mag-Bind Soil DNA Kit (Omega Bio-Tek, USA). Concentration and purity were determined using NanoDrop 2000 (Thermo Scientific, USA). DNA was amplified according to the V3-V4 region of the bacterial 16S rRNA gene by using the T100 Thermal Cycler (BIO-RAD, USA) and bacterial primers: 338F (5′-ACTCCTACGGGGGAGGCAGCAG-3′) and 806R (5′-GGACTACHVGGGTWTCTAAT-3′). DNA libraries were constructed using the NEXTFLEX Rapid DNA Sequencing Kit (Bioo Scientific, USA) and sequenced using the Illumina PE250 platform (Illumina, USA). This process provided the representative amplicon sequence variant (ASV) and abundance data.

Bioinformatics analysis was performed using the Majorbio cloud platform (www.majorbio.com). Core and sparse curves were employed to ensure that the sample size or sequencing depth was saturated. The Wilcoxon rank-sum test was performed to assess differences in the alpha diversity index between the groups. Based on the beta diversity distance matrix, Hierarchical clustering analysis was performed to illustrate the microbiota variation between the groups. Venn diagrams were plotted to quantify the shared and unique species among the groups. The similarity of the microbiota structure between the groups was examined through principal co-ordinate analysis (PCoA), which was based on Bray-Curtis. The linear discriminant analysis (LDA) and effect size (LEfSe) (LDA > 3, $P < 0.05$) highlighted the species information that best explained the differences between the groups.

Targeted LC-MS Metabolomic Analysis

Lower airway secretions and plasma samples were chromatographically separated on a Waters ACQUITY UPLC HSS T3 column (Waters, USA) by using an EXIONLC System (SCIEX, USA) for ultra-high-performance liquid chromatography (UHPLC). The SCIEX 6500 QTRAP+ triple quadrupole mass spectrometer (SCIEX, USA), equipped with the IonDrive Turbo V electrospray ionization interface, was employed in the multiple reaction monitoring (MRM) mode for assay development. Mass spectrometry (MS) data were quantified using SCIEX Analyst Work Station Software (version 1.6.3) and SCIEX MultiQuant software (version 3.0.3). A total of 31 tryptophan metabolic pathway-related target metabolites were quantified in lower airway secretions and plasma samples by using UHPLC-MRM-MS/MS.

Using SIMCA software (V16.0.2, Umea, Sweden), the principal component analysis (PCA) of metabolites was conducted on samples from different groups. The data were further analyzed through orthogonal partial least squares-discriminant analysis (OPLS-DA), validated by 7-fold cross-validation to judge model validity based on R^2Y and Q^2 values. Permutation tests confirmed model effectiveness, ensuring reliable group differentiation. Univariate and multivariate analyses were performed using the metabolites, with volcano plots illustrating upregulated and downregulated metabolites. Matchstick plots were applied to indicate significant differences in metabolites between the groups.

Correlation Analysis Between Microbiota and Tryptophan Metabolites

A correlation heatmap analysis was conducted using the Pearson coefficient to assess the correlation between the changes in the microbiota and metabolites. $P < 0.05$ was considered to indicate a significant correlation.

Model Diagnostic Prediction Analysis

The area under the curve (AUC) from the receiver operating characteristic (ROC) curve was calculated to evaluate the diagnostic predictive ability of the altered microbiota and tryptophan metabolites for NARDS.

Statistical Analysis

All data were analyzed using SPSS version 25.0 software (SPSS Inc., USA). Normally distributed data were presented as mean ± standard deviation and evaluated using independent *t*-tests or one-way ANOVA. Non-normally distributed data were presented using the median (interquartile range) and evaluated using non-parametric tests. Count data were assessed using chi-square tests, continuity-corrected chi-square tests, or Fisher's exact tests. All statistical tests were two-sided, and $P < 0.05$ was considered significant.

Results

Clinical Characteristics

Figure 1 illustrates the flowchart of patient enrollment in the study. The study included 50 neonates, including 25 NARDS neonates in the NARDS group and 25 NRDS or TTN neonates in the control group. In addition, the NARDS group included 15 newborns with moderate to severe NARDS in the NARDS_S group and 10 newborns with mild NARDS in the NARDS_M group.

Table 1 presents demographic and clinical characteristics. The NARDS group had an average gestational age, a median weight, and a median postnatal age at admission of 35.14 weeks, 2800 g, and 2 h, respectively. This group included 40% female infants, 76% cesarean deliveries, and 64% formula-fed infants. The NARDS group exhibited median durations of 11 days for total ventilator ventilation time, 17 days for total oxygen time, and 25 days for hospitalization time. There was no significant difference in the basic conditions and risk factors between the two groups. However, because the condition of newborns in the NARDS group was more severe than that in the control group, the duration of ventilator ventilation, total oxygen use, and hospital stay were longer. In addition, all children in both groups recovered and were discharged, except for one NARDS patient who stopped treatment due to financial reasons. There were no significant differences in the characteristics of newborns between the NARDS_S and NARDS_M groups, except for differences in the age at sampling, total duration of oxygen therapy, and length of hospital stay.

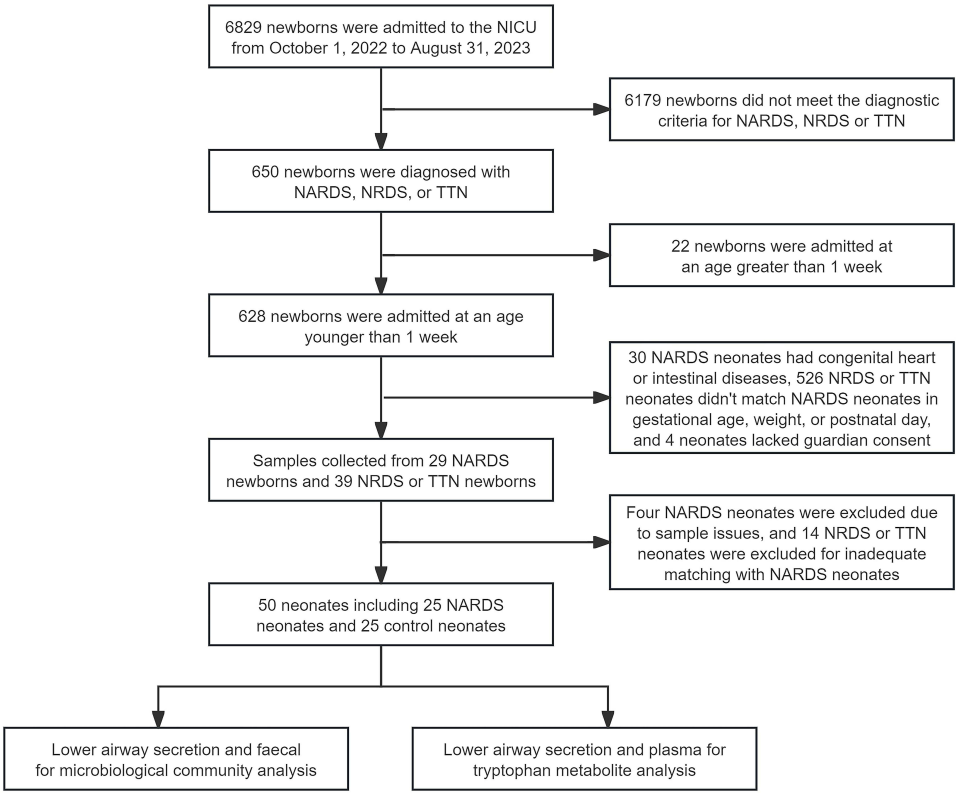

Figure 1 Flowchart of patient enrollment in the study.
Abbreviations: NICU, neonatal intensive care unit; NARDS, neonatal acute respiratory distress syndrome; NRDS, neonatal respiratory distress syndrome; TTN, transient tachypnea of the newborn.

Microbiome Analysis

Changes in the Lung Microbiota of NARDS

A total of 5,363,981 high-quality 16S rDNA reads (average length 425 bps) were obtained from the 50 lower airway secretion samples. Core curves revealed consistent core species regardless of sample size increase, indicating sufficient sample sequencing (Figure S1a). ACE and Shannon index rarefaction curves reached a plateau at the ASV level, confirming adequate sequencing depth (Figure S1b).

The Venn diagram revealed 272 OTUs common to the NARDS and control groups, with 1362 and 1998 unique OTUs in the NARDS and control groups, respectively (Figure S1c). Hierarchical clustering analysis highlighted marked differences in

Table 1 Demographic and Clinical Characteristics of the Study Population

Characteristics and Outcome	NARDS (n=25)				Control (n=25)	P
	Total (n=25)	NARDS_S (n=15)	NARDS_M (n=10)	p		
Female n,(%)	10 (40%)	7 (47%)	3 (30%)	0.68	13 (52%)	0.40
Postnatal age at admission (h) (IQR)	2.00 (1.50–10.50)	2.00 (1.00–13.00)	2.00 (1.75–10.00)	0.82	2.00 (1.00–2.50)	0.06
Age of sample collection (d) (IQR)	1.00 (1.00–3.00)	2.00 (1.00–3.00)	1.00 (1.00–1.00)	<0.01	2.00 (1.00–3.00)	0.88
Birth weight (g) (IQR)	2800.00 (1660.00–3397.50)	2655.67 ±954.92	2421.00 ±955.01	0.55	2720.00 (1765.00–3150.00)	0.57
Gestational age (wk)	35.14 ± 3.81	35.01 ± 3.95	35.33 ± 3.77	0.85	35.84 ± 3.20	0.49
Cesarean delivery n,(%)	19 (76%)	11 (85%)	8 (80%)	1.00	16 (68%)	0.53
Formula-fed (%)	16 (64%)	8 (53%)	2 (20%)	0.21	20 (80%)	0.21
OI (IQR)	8.00 (6.00–13.00)	11.00 (9.00–25.00)	5.50 (4.75–7.00)	<0.01	/	/

(*Continued*)

Table 1 (Continued).

Characteristics and Outcome	NARDS (n=25)				Control (n=25)	P
	Total (n=25)	NARDS_S (n=15)	NARDS_M (n=10)	p		
Risk factors						
Grade III meconium-stained amniotic fluid n,(%)	3 (12%)	2 (13%)	2 (20%)	1.00	3 (12%)	1.00
Premature rupture of membranes >18 hours n,(%)	3 (12%)	3 (20%)	0 (0%)	0.25	7 (28%)	0.16
Fetal distress n,(%)	3 (12%)	2 (13%)	0 (0%)	0.50	2 (8%)	1.00
Antepartum infection n,(%)	5 (20%)	3 (20%)	2 (20%)	1.00	2 (8%)	0.41
Use of antepartum antibiotics n,(%)	6 (24%)	3 (20%)	3 (30%)	0.65	5 (20%)	0.73
Gestational hypertension n,(%)	4 (16%)	1 (7%)	3 (30%)	0.27	3 (12%)	1.00
Gestational diabetes n,(%)	4 (16%)	2 (13%)	2 (20%)	1.00	4 (16%)	1.00
Gestational cholestasis n,(%)	3 (12%)	2 (13%)	2 (20%)	1.00	3 (12%)	1.00
Triggers of NARDS						
Sepsis n,(%)	12 (48%)	9 (60%)	2 (20%)	0.09	/	/
Pneumonia n,(%)	6 (24%)	3 (20%)	3 (30%)	0.65	/	/
Perinatal asphyxia n,(%)	4 (16%)	2 (13%)	3 (30%)	0.36	/	/
Meconium aspiration n,(%)	3 (12%)	1 (6%)	2 (20%)	0.54	/	/
Treatments						
Antibiotic use n,(%)	12 (48%)	9 (60%)	3 (30%)	0.23	10 (40%)	0.57
Invasive ventilation duration n,(%)	18 (72%)	15 (100%)	9 (90%)	0.40	0 (0%)	<0.01
Non-invasive ventilation duration n,(%)	24 (96%)	11 (73%)	7 (70%)	1.00	9 (36%)	<0.01
Outcome						
Total duration of ventilator use (d) (IQR)	11.00 (6.00–25.00)	12.00 (7.00–39.00)	7.50 (5.50–20.00)	0.08	0.00 (0.00–4.50)	<0.01
Total oxygen therapy duration (d) (IQR)	17.00 (9.50–35.50)	30.00 ± 19.10	12.80 ± 8.26	<0.01	8.00 (3.00–16.50)	<0.01
BPD n,(%)	5 (20%)	3 (20%)	2 (20%)	1.00	1 (4%)	0.19
ROP n,(%)	1 (4%)	1 (7%)	0 (0%)	1.00	0 (0%)	1.00
NICU stay (d) (IQR)	25.00 (15.50–46.00)	35.93 ± 17.59	18.70 ± 10.60	<0.01	16.00 (9.00–35.00)	0.04

Note: The summary statistic is expressed as number (%), mean ± sd or median (25th-75th percentiles).
Abbreviations: NARDS, Neonatal acute respiratory distress syndrome; NARDS_S, moderate-to-severe NARDS; NARDS_M, mild NARDS; IQR, Interquartile Range; wk, week; BPD, Bronchopulmonary Dysplasia; ROP, Retinopathy of Prematurity; NICU, Neonatal Intensive Care Unit.

the colonization of bacteria in the lower airway secretions between the groups (Figure 2a). PCoA revealed significant differences in the microbial community structure in the lower airway secretions between the NARDS and control groups (R = 0.211, $P = 0.001$, Figure 2b). The microbial composition in the lower airway secretions differed significantly between the NARDS and control groups. At the phylum level, the NARDS group was dominated by *Proteobacteria* (67.83%), *Bacteroidota* (17.02%), and *Fir*micutes (9.90%). The control group consisted mainly of *Firmicutes* (48.91%), *Proteobacteria* (29.56%), and *Actinobacteriota* (10.79%). At the genus level, *Achromobacter* (55.81%), and *Pedobacter* (14.43%) dominated the NARDS group. The control group was characterized by *Streptococcus* (35.72%), *Achromobacter* (22.36%), *Staphylococcus* (10.36%) (Figure 2c). Differential analysis and LEfSe (LDA = 3, $P < 0.05$) revealed significant disparities at both phylum and genus levels between the NARDS and control groups. The NARDS group exhibited significantly higher abundances of *Proteobacteria* and *Bacteroidota* and lower abundances of *Firmicutes* at the phylum level. At the genus level, the abundances of *Achromobacter, Pedobacter, Pseudomonas, Lawsonella, Friedmanniella, Delftia, Cutibacterium, Cloacibacterium, Sphingobacterium, and Rhodobacteraceae* significantly increased, whereas *Streptococcus* and *Rothia* significantly decreased ($P < 0.05$, Figure 2d and e).

In total, 145 OTUs were shared between the NARDS_S and NARDS_M groups, with 761 and 728 unique OTUs in the two groups, respectively (Figure S1d). The LEfSe (LDA = 3, $P < 0.05$) found no significant phylum-level differences but observed a significant reduction in the abundance of *Lactobacillus* at the genus level in the NARDS_S group (Figure 2f).

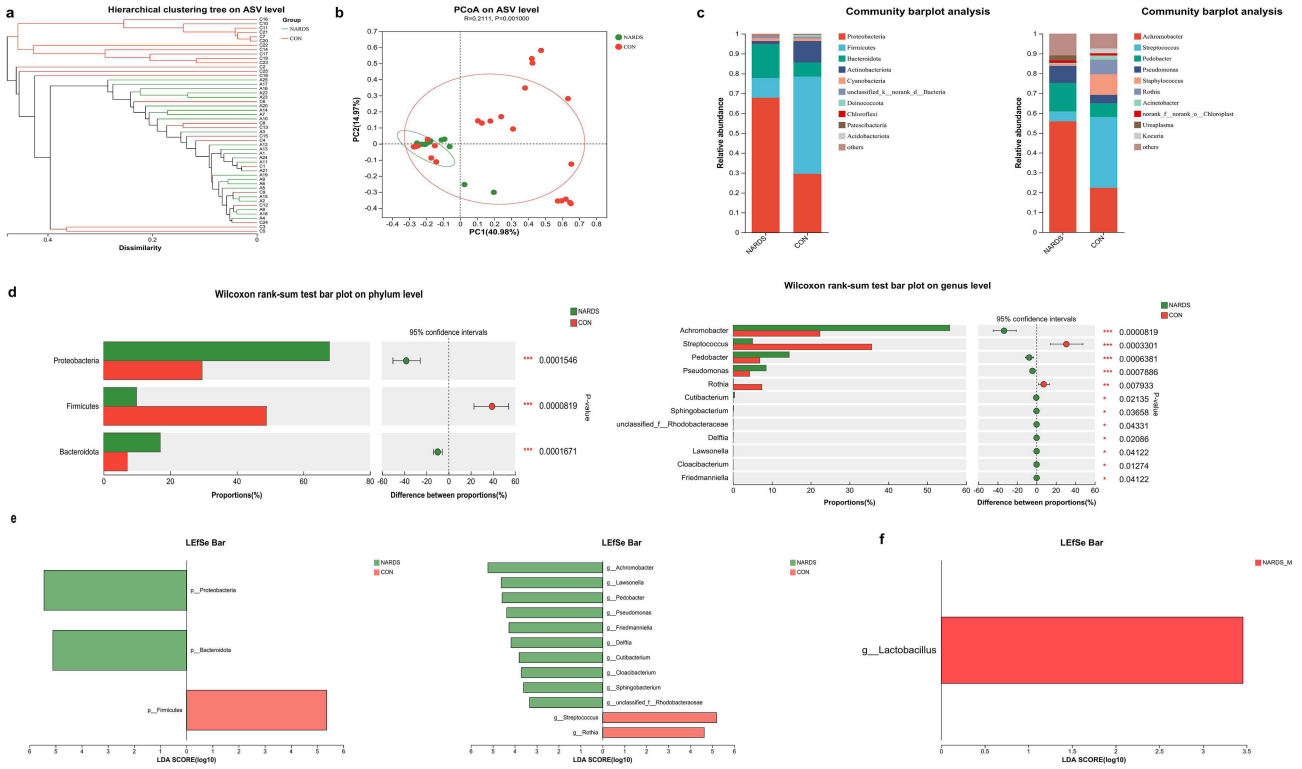

Figure 2 Microbial Composition and Diversity Analysis in Lower Airway Secretions. (**a**) Hierarchical clustering analysis visualization depicting significant differences in the microbial composition between the NARDS and control groups. (**b**) PCoA analysis revealed significant differences in the microbiota of lower airway secretions between the NARDS and control groups (R = 0.211, *P* = 0.001). PC1 indicates the variation of samples along the first principal component, and PC2 represents the variation along the second principal component. (**c**) Demonstration of the microbial structure of lower airway secretions from the NARDS and control groups at the phylum and genus levels. (**d**) Differential analysis between the NARDS and control groups highlights significantly different bacteria in the lower airway secretions at both the phylum and genus levels (*0.01 < *P* ≤ 0.05, **0.001 < *P* ≤ 0.01, ***P* ≤ 0.001). (**e**) LEfSe analysis showed the most significant differences in the lower airway secretions between the NARDS and control groups at the phylum and genus levels. (**f**) LEfSe analysis identifies the most significantly different bacteria in the lower airway secretions between the NARDS_S and NARDS_M groups.

Abbreviations: NARDS, neonatal acute respiratory distress syndrome; CON, control; NARDS_S, moderate-to-severe NARDS; NARDS_M, mild NARDS; PCOA, principal co-ordinate analysis; ASV, amplicon sequence variant; LEfSe, linear discriminant analysis effect size.

Changes in the Gut Microbiota of NARDS

Analyzing 50 fecal samples yielded 5,990,534 high-quality 16S rDNA reads (average length 417 bps). Core curves indicated sufficient sample size, and ACE and Shannon index rarefaction curves confirmed appropriate sequencing depth (Figure S2a and b).

The Venn diagram revealed 442 shared OTUs between NARDS and control groups, with 1447 and 1201 unique OTUs in the NARDS and control groups, respectively (Figure S2c). Hierarchical clustering analysis does not provide a direct visualization of the disparities in fecal community composition between the NARDS and control group (Figure 3a). PCoA highlighted significant differences in the fecal microbial structure of the NARDS and control groups (R = 0.0486, *P* = 0.038, Figure 3b). *Proteobacteria* and *Firmicutes* were predominant in both groups (> 90% of total bacteria), with significantly higher *Deferribacterota* abundance in the NARDS group (*P* < 0.05, Figure 3c and d). At the genus level, the fecal microbiota in the NARDS group was characterized by higher abundances of *Novosphingobium* (16.79%), *Streptococcus* (13.56%), *Methylobacterium-Methylorubrum* (13.33%). The fecal microbiota in the control group predominantly included *Enterococcus* (23.68%), *Novosphingobium* (16.11%), *Methylobacterium-Methylorubrum* (11.31%) (Figure 3c). The NARDS group exhibited significant increases in the abundances of *Mucispirillum, Roseburia, Intestinimonas, and Anaerococcus* and decreases in the abundance of *Enterococcus* (*P* < 0.05, Figure 3d and e).

A comparative analysis of fecal microbiota between the NARDS_S and NARDS_M groups revealed 179 shared OTUs, with 857 and 853 unique OTUs in the NARDS_S and NARDS_M groups, respectively (Figure S2d). At the genus level, the NARDS_S group had significantly higher abundances of *Streptococcus, Lactococcus*, and *Kocuria*, while

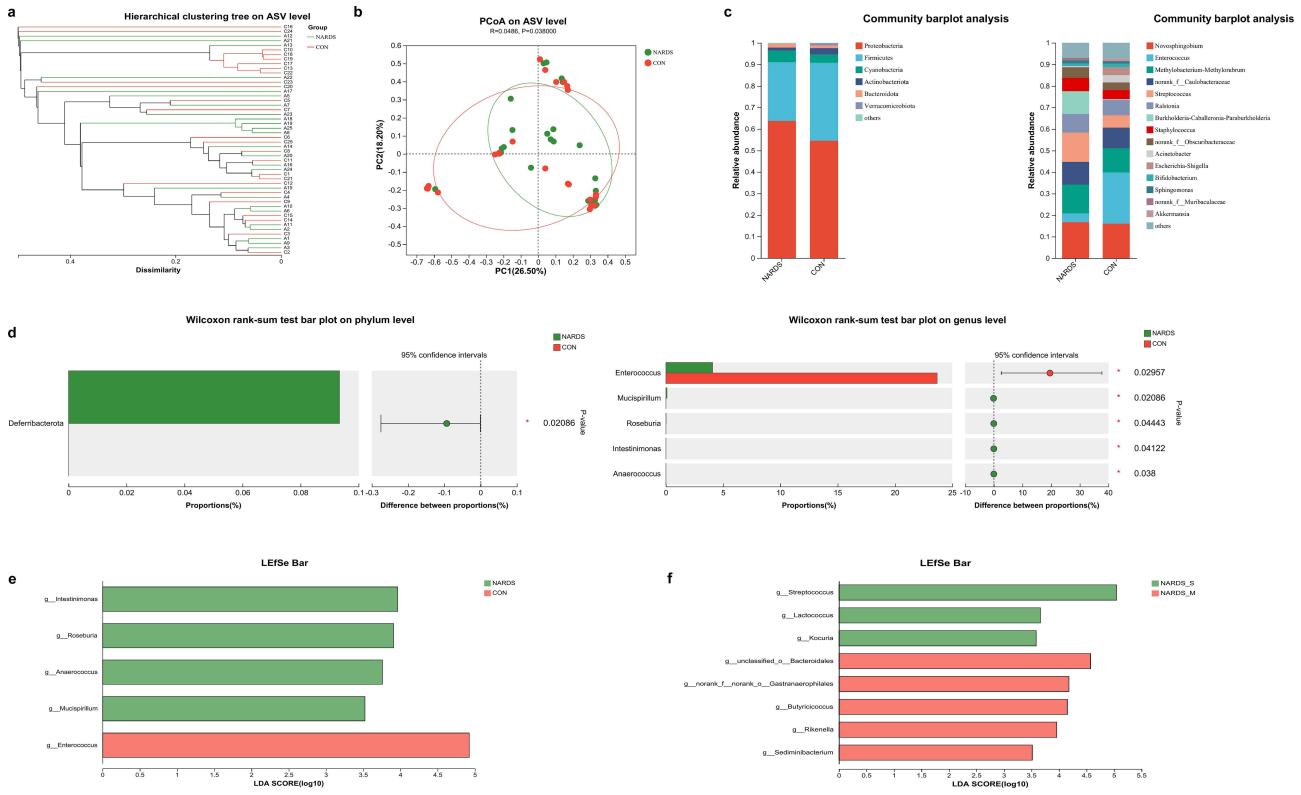

Figure 3 Microbial Structure and Diversity Analysis in Feces. (**a**) Hierarchical cluster analysis visualized differences in microbial composition of feces between NARDS and control groups. (**b**) PCoA analysis showed significant differences in the microbiota of feces between the NARDS and control group (R = 0.0486, *P* = 0.038). PC1 indicates the variation of samples along the first principal component, and PC2 represents the variation along the second principal component. (**c**) Demonstration of the microbial structure of feces from the NARDS and control groups at the phylum and genus levels. (**d**) Differential analysis between the NARDS and control groups highlights significantly different bacteria in feces at both the phylum and genus levels (*0.01 < *P* ≤ 0.05). (**e**) LEfSe analysis showed the most significant differences in the feces between the NARDS and control groups. (**f**) LEfSe analysis identifies the most significantly different bacteria in the the feces between the NARDS_S and NARDS_M groups.
Abbreviations: NARDS, neonatal acute respiratory distress syndrome; CON, control; NARDS_S, moderate-to-severe NARDS; NARDS_M, mild NARDS; PCOA, principal co-ordinate analysis; ASV, amplicon sequence variant; LEfSe, linear discriminant analysis effect size; LDA, linear Discriminant Analysis.

abundances of *Sediminibacterium, Rikenella, Butyricicoccus, Gastranaerophilales*, and *Bacteroidales* were significantly lower ($P < 0.05$, Figure 3f).

Metabolomic Analysis

Changes in Lung Tryptophan Metabolites in NARDS Patients

In total, 21 metabolites were detected in the lower airway secretions. The PCA unveiled the distribution and dispersion of samples between the NARDS and control groups, with principal components PC1 and PC2 accounting for 49.2% and 12%, respectively (Figure 4a). The OPLS-DA and 7-fold cross-validation confirmed significant metabolomic differences, validated by permutation tests (R^2Y=0.549, Q^2=0.404) (Figure 4b and c).

The volcano plots presented the differences in tryptophan metabolites between the NARDS and control groups. In the NARDS group, 6 metabolites were downregulated, whereas 15 metabolites were upregulated (Figure 4d). Seven metabolites showed significant changes, including increased levels of 5-hydroxyindoleacetic acid (5-HIAA), 5-hydroxytryptophol (5-HTOL), ILA, and kynurenic acid (KYNA), and decreased levels of nicotinic acid, xanthurenic acid (Xa), and ICA ($P <$ 0.05, Figure 4e). Notably, metabolites linked to microbial metabolism, such as ILA and ICA, exhibited significant alterations. Moreover, the kynurenine/tryptophan (KYN/Trp) ratio was significantly increased in the NARDS group ($P < 0.05$).

A comparative analysis of metabolites in the lower airway secretions between the NARDS_S and NARDS_M groups identified nine differentially abundant tryptophan metabolites. In the NARDS_S group, the levels of 3-hydroxykynurenine (3-HK), 5-HIAA, indoleacetic acid (IAA), ILA, IPA, indoxyl sulfate (IS), KYN, and Trp were lower, while indole-

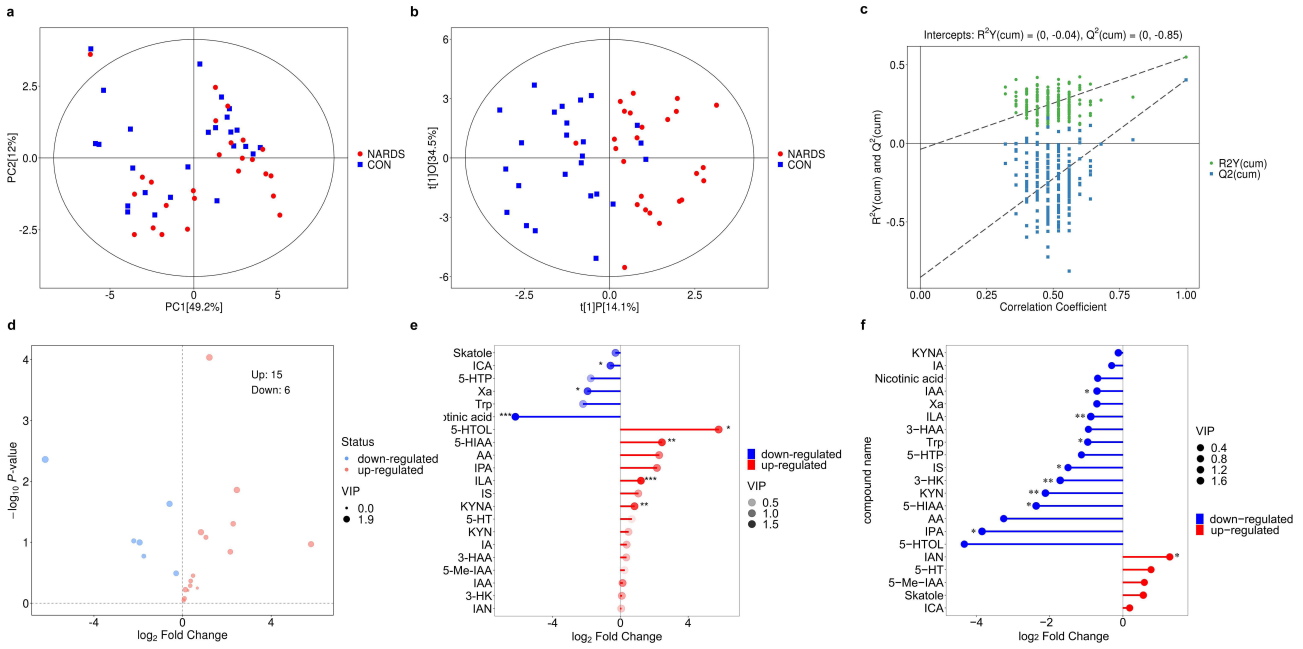

Figure 4 Tryptophan Metabolite Analysis in Lower Airway Secretions. (**a**) The PCA Score Plot illustrated the distribution of the lower airway secretion samples. The X-axis (PC[1]) and Y-axis (PC[2]) represented the first and second principal components, respectively, indicating the explained variance. Each dot represented a sample. (**b**) The OPLS-DA Score Plot demonstrated the separation of groups. The X-axis (t[1]P) displayed the predictive component scores of the first principal component, highlighting differences between groups, while the Y-axis (t[1]O) showed the orthogonal component scores, elucidating variances within groups. Each point represented a sample. (**c**) Permutation test for the OPLS-DA model, with the X-axis denoting permutation iterations and the Y-axis showing the values of R^2Y and Q^2. R^2Y (green circles) and Q^2 (blue squares) respectively indicate the goodness of fit and predictive ability of the model, with dashed lines representing regression lines for R^2Y and Q^2. (**d**) Volcano Plot for Tryptophan Metabolites compared the NARDS group to the control group, where red dots represented upregulated metabolites and blue dots indicated downregulated metabolites. (**e**) Matchstick Plot for tryptophan metabolites contrasted the NARDS group with the control group (*0.01 < P < 0.05, **0.001 < P < 0.01, ***P < 0.001). (**f**) Matchstick Plot contrasting the NARDS_S group with the NARDS_M group (*0.01 < P < 0.05, **0.001 < P < 0.01).

Abbreviations: NARDS, neonatal acute respiratory distress syndrome; CON, control; NARDS_S, moderate-to-severe NARDS; NARDS_M, mild NARDS; PCA, the principal component analysis; OPLS-DA, orthogonal partial least squares-discriminant analysis; VIP, variable importance in the projection.

3-acetonitrile (IAN) increased (Figure 4f). Notably, except for 5-HIAA, all these metabolites, closely tied to microbial metabolism, showed significant differences ($P < 0.05$).

Changes in Plasma Tryptophan Metabolites in NARDS Patients

In total, 22 metabolites were observed in the plasma sample. The PCA exhibited the distribution and dispersion of samples between the NARDS and control groups, with PC1 and PC2 accounting for 51.4% and 14.2%, respectively (Figure 5a). The OPLS-DA scatter plots exhibited no significant overall differences in metabolites between the NARDS and control groups (Figure 5b). The OPLS-DA permutation test yielded $R^2Y = 0.389$ and $Q^2 = -0.052$ (Figure 5c).

The volcano plots reveal that 10 tryptophan metabolites are downregulated, and 12 tryptophan metabolites are upregulated in the NARDS group (Figure 5d). The plasma levels of anthranilic acid (AA), ILA, and KYNA were significantly increased in the NARDS group. ILA is closely related to microbial metabolism ($P < 0.05$, Figure 5e). Additionally, the KYN/Trp ratio significantly increased in the plasma samples in the NARDS group ($P < 0.05$).

Differential analysis in the NARDS_S and NARDS_M groups identified two significant metabolites: plasma levels of KYN decreased, while IAA increased in the NARDS_S group; both metabolites were associated with microbial metabolism ($P < 0.05$, Figure 5f).

Significant Correlation Between the Altered Microbiota and Tryptophan Metabolites

Pearson's correlation analysis revealed the correlations between the top five differentially abundant genera in the lungs *(Achromobacter, Pedobacter, Streptococcus, Pseudomonas, Rothia* for NARDS and the control group; *Lactobacillus, Stenotrophomonas* for NARDS_S and NARDS_M groups) and tryptophan metabolites (ICA, ILA for NARDS and the control group; 3-HK, IAA, IAN, ILA, IPA, IS, KYN, Trp for NARDS_S and NARDS_M groups). In the NARDS group,

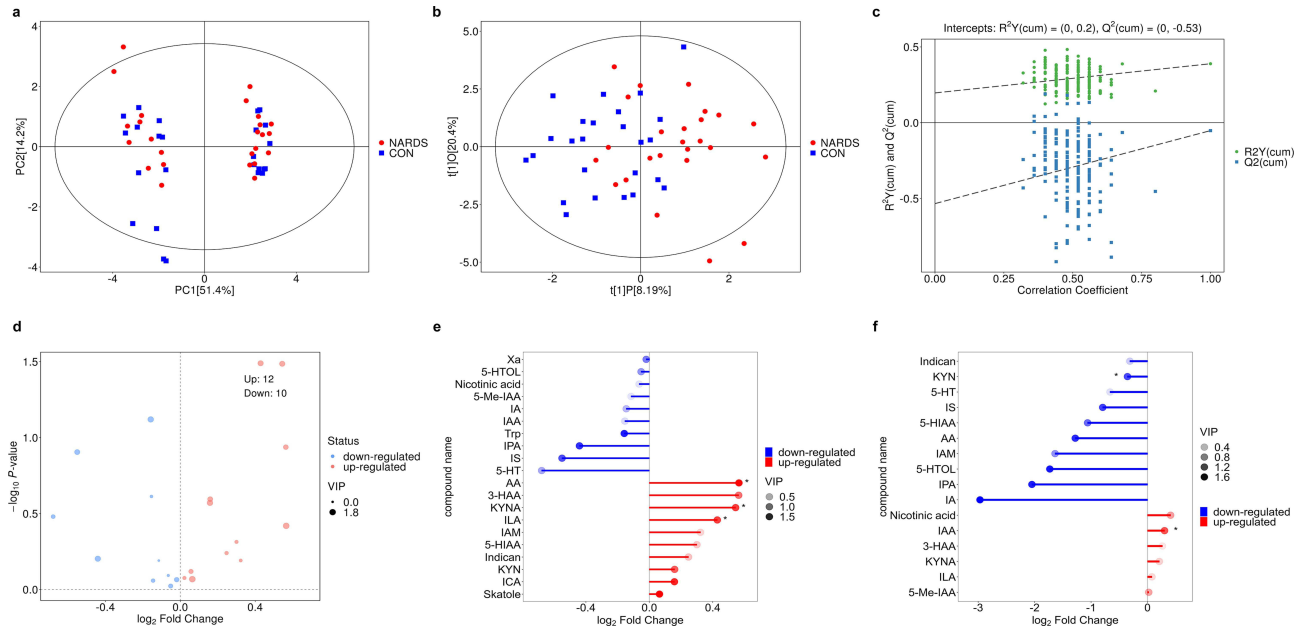

Figure 5 Tryptophan Metabolite Analysis in Plasma. (**a**) The PCA Score Plot illustrated the distribution of the plasma samples. The X-axis (PC[1]) and Y-axis (PC[2]) represented the first and second principal components, respectively, indicating the explained variance. Each dot represented a sample. (**b**) The OPLS-DA Score Plot demonstrated the separation of groups. The X-axis (t[1]P) displayed the predictive component scores of the first principal component, highlighting differences between groups, while the Y-axis (t[1]O) showed the orthogonal component scores, elucidating variances within groups. Each point represented a sample. (**c**) Permutation test for the OPLS-DA model, with the X-axis denoting permutation iterations and the Y-axis showing the values of R^2Y and Q^2. R^2Y (green circles) and Q^2 (blue squares) respectively indicate the goodness of fit and predictive ability of the model, with dashed lines representing regression lines for R^2Y and Q^2. (**d**) Volcano Plot for Tryptophan Metabolites compared the NARDS group to the control group, where red dots represented upregulated metabolites and blue dots indicated downregulated metabolites. (**e**) Matchstick Plot for tryptophan metabolites contrasted the NARDS group with the control group (*0.01 < P < 0.05). (**f**) Matchstick Plot contrasting the NARDS_S group with the NARDS_M group (*0.01 < P < 0.05).

Abbreviations: NARDS, neonatal acute respiratory distress syndrome; CON, control; NARDS_S, moderate-to-severe NARDS; NARDS_M, mild NARDS; PCA, the principal component analysis; OPLS-DA, orthogonal partial least squares-discriminant analysis; VIP, variable importance in the projection.

the decreased abundance of *Streptococcus* in lower airway secretions was negatively correlated with increased ILA levels. Conversely, the increased abundance of *Pseudomonas* was negatively correlated with decreased ICA levels. Higher abundances of *Achromobacter* and *Pedobacter* were positively correlated with elevated ILA levels ($P < 0.05$, Figure 6a). In the NARDS_S group, the reduced abundances of *Lactobacillus* and *Stenotrophomonas* were positively correlated with decreased IPA levels. Additionally, the reduced abundance of *Rhodobacteraceae* was positively correlated with the decreased HK and ILA levels ($P < 0.05$, Figure 6b).

Given the substantial microbial community of the gut, modifications in the gut microbiota can alter intestinal tryptophan metabolites, influencing other organs through the bloodstream or lymphatic circulation.[6] As the gut microbiota is approximately 10 times larger than the lung microbiota, alterations in circulating microbe-associated tryptophan metabolites are primarily attributed to modifications in intestinal metabolites.[8,31,32] The correlation between the top 5 differentially abundant genera in feces (*Enterococcus* for NARDS and the control group; *Streptococcus* for NARDS_S and NARDS_M groups) and tryptophan metabolites in plasma (ILA for NARDS and the control group; IAA, KYN for NARDS_S and NARDS_M groups) was assessed using Pearson correlation analysis. Consequently, no significant correlations were observed between differential fecal bacteria and differential plasma tryptophan metabolites in the NARDS and control groups (Figure 6c). However, on analyzing differential fecal bacteria and plasma tryptophan metabolites in the NARDS_S and NARDS_M groups, increased abundances of *Lactococcus* and *Kocuria* were positively correlated with higher IAA concentrations in the NARDS_S group ($P < 0.05$, Figure 6d).

Changes in Lung Microbiota and Tryptophan Metabolites Have a Better Differentiated Ability for NARDS

Based on the top five differentially abundant genera in the lung and intestine, as well as all differential tryptophan metabolites associated with microbial metabolism in the lung and plasma, ROC plots were constructed to determine their

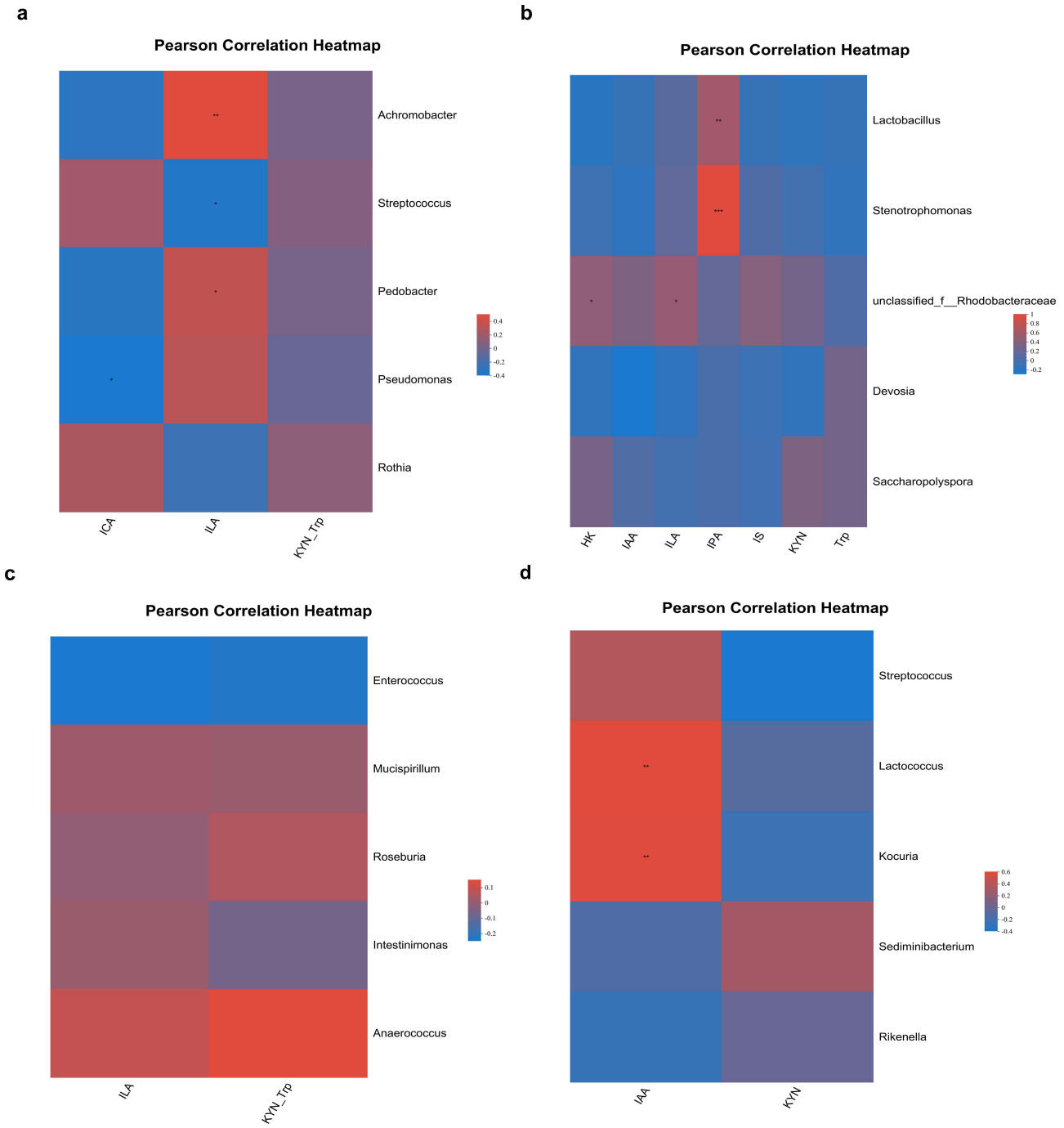

Figure 6 Correlation Analysis between Differential Genera and Tryptophan Metabolites. (**a**) Correlation analysis between distinct bacterial flora and varying tryptophan metabolites in the lower airway secretions of the NARDS and control groups. (**b**) Correlation analysis between diverse bacterial flora and different tryptophan metabolites in the lower airway secretions of the NARDS_S and NARDS_M groups. (**c**) Correlation analysis between varied fecal flora and different tryptophan metabolites in the plasma of NARDS and control groups. (**d**) Correlational analysis between distinct fecal flora and plasma tryptophan metabolites in the NARDS_S group and the NARDS_M group. (*$0.01 < P \leq 0.05$, **$0.001 < P \leq 0.01$, ***$P \leq 0.001$, red indicates a positive correlation, while blue signifies a negative correlation).

Abbreviations: ICA, indole-3-carboxaldehyde; ILA, indoleacetic acid; KTN_Trp, kynurenine/ tryptophan; HK, 3-hydroxykynurenine; IAA, indoleacetic acid; IAN, indole-3-acetonitrile; IPA, 3-indole propionic acid; IS, indoxyl sulfate; KYN, kynurenine; Trp, tryptophan; NARDS, neonatal acute respiratory distress syndrome; NARDS_S, moderate-to-severe NARDS; NARDS_M, mild NARDS.

potential diagnostic values for NARDS. AUC values exceeding 0.5 indicate predictive significance, with improved diagnostic accuracy as the AUC approaches 1. Conversely, AUC values of ≤ 0.5 suggest no diagnostic value.

The ROC plots were generated using the top five differentially abundant genera and all differential tryptophan metabolites in the lungs for the NARDS and control groups, as well as the NARDS_S and NARDS_M groups, which

exhibited AUC values of 0.78 and 0.8, respectively. This suggests that the abundance of these genera and metabolites in the lungs can predict NARDS and its severity (Figure 7a and b). However, the ROC plots constructed using the top five differentially abundant genera in the gut and all differential tryptophan metabolites in plasma samples for the NARDS and control groups, as well as the NARDS_S and NARDS_M groups, demonstrated AUC values of 0.5 and 0.45, respectively. This indicates that differential gut genera and plasma tryptophan metabolites have no predictive value for NARDS diagnosis or severity (Figure 7c and d).

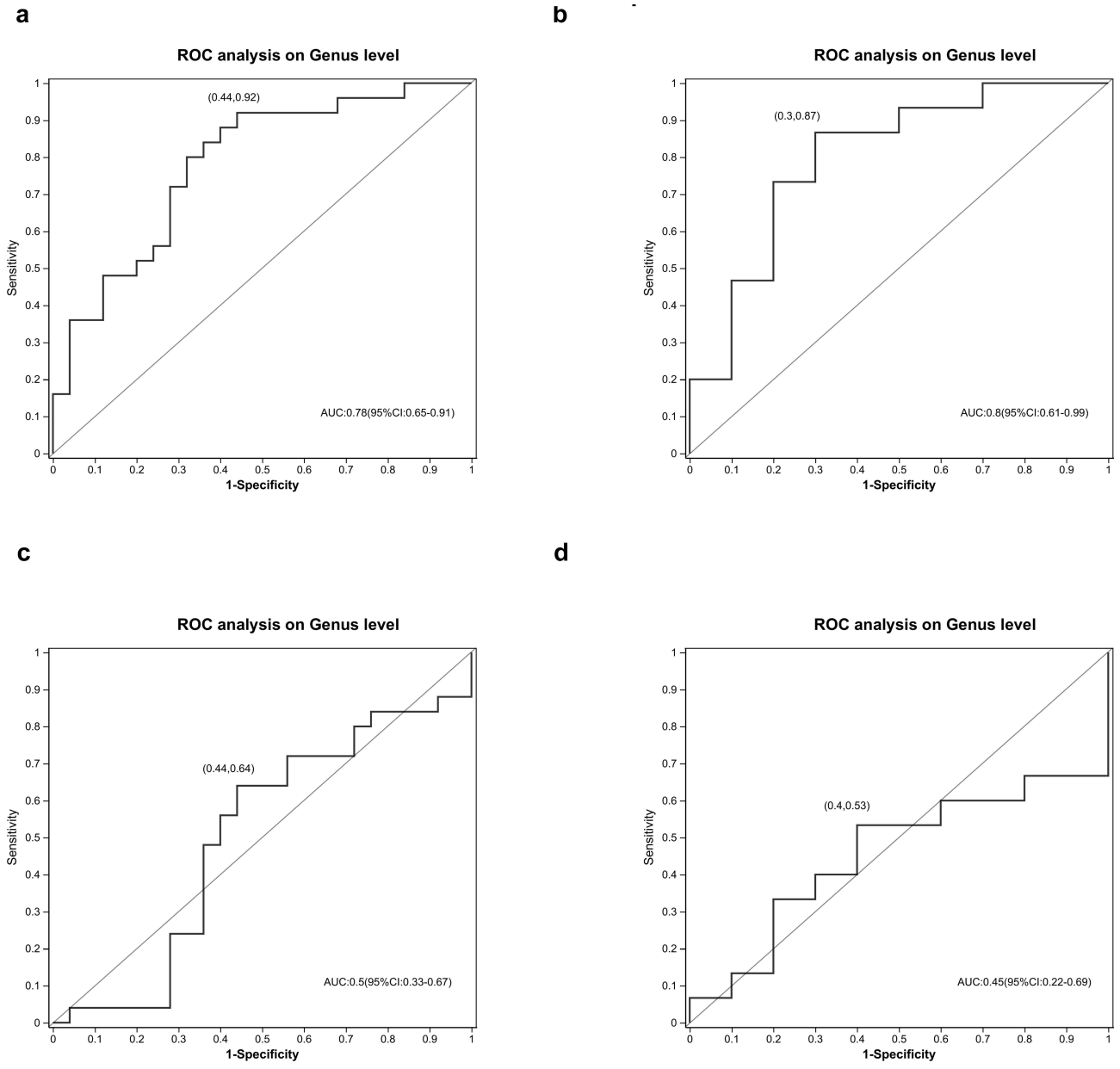

Figure 7 ROC Curve Analysis based on Differential Genera and Tryptophan Metabolites. (**a**) ROC plotted according to differential genera and tryptophan metabolites in the lower airway secretions comparing the NARDS group with the control group. (**b**) ROC analysis based on differential genera and tryptophan metabolites in the lower airway secretions between the NARDS_S and NARDS_M groups. (**c**) ROC curves were constructed using differential genera in feces and tryptophan metabolites in plasma of NARDS and control groups. (**d**) ROC analysis utilizing differential genera in feces and tryptophan metabolites in plasma between the NARDS_S and NARDS_M groups. (The X-axis represents 1-specificity and the Y-axis indicates sensitivity. Marked points on the curves signify optimal thresholds.).

Abbreviations: ROC, receiver operating characteristic; AUC, area under the curve; NARDS, neonatal acute respiratory distress syndrome; NARDS_S, moderate-to-severe NARDS; NARDS_M, mild NARDS.

Discussion

For the first time, we employed microbiomics and targeted metabolomics to explore the lung-gut microbiome and lung-plasma metabolomics in NARDS patients. Significant changes were detected in both the lung-gut microbiota and lung-plasma tryptophan metabolites.

The lungs, once considered sterile, harbor extensive microbial communities in healthy individuals.[33] According to our research findings, the lower airway secretion microbiota exhibits significantly different characteristics in NARDS patients compared to the control group. We observed a significant increase in *Proteobacteria* and *Bacteroidota*, coupled with a decrease in *Firmicutes* in the lungs of NARDS patients, consistent with findings in respiratory diseases.[34,35] Both *Proteobacteria* and *Bacteroidota* have pro-inflammatory properties and may play a role in lung tissue remodeling and promoting lung injury processes.[36–38] Additionally, certain *Firmicutes* genera have established anti-inflammatory properties. The decline in *Firmicutes*, along with an increase in *Proteobacteria* and *Bacteroidota*, is closely associated with inflammatory diseases.[39,40] Therefore, dysbiosis in the microbial composition may lead to an imbalance in barrier homeostasis and inflammation. In particular, we observed a significant decrease in *Streptococcus* and *Rothia* at the genus level in the NARDS patients. The reduction in *Streptococcus* is negatively correlated with the progression and severity of lung diseases, potentially indicating dysbiosis in the respiratory microbiota of NARDS patients.[41] Additionally, the abundance of *Rothia* is negatively correlated with pro-inflammatory markers in sputum, possibly alleviating inflammation by inhibiting the activation of the NF-κB pathway.[42] Surprisingly, we found a significant reduction in the abundance of *Lactobacillus* in lower airway secretions in the NARDS_S group. Previous studies have shown that *Lactobacillus*, with components such as peptidoglycan and extracellular polysaccharides, plays a regulatory role in respiratory immunity and has beneficial effects in respiratory diseases such as infections, asthma and chronic obstructive pulmonary disease (COPD).[43–47] In recent years, "bacterial therapy" has gradually gained attention, with saliva-derived *Streptococcus 24SMB* and oral *Streptococcus 89a* being applied in the clinical treatment of respiratory diseases.[48] Therefore, modifications in lung microbiota may predict disease progression and prognosis, and intervention with key lung microbiota bacteria could be an effective treatment for NARDS patients.

The "gut-lung axis" is a crucial mechanism through which gut microbiota influence lung diseases.[7] In neonates, the acute phase of NARDS typically occurs within the first 3 days of life.[26] The gut microbiota in early neonates, influenced by birth mode, feeding, and environment, displays low diversity, simple functionality, rapid changes, and significant individual differences.[28] In our study, *Proteobacteria* and *Firmicutes* dominated the fecal microbiota in both NARDS and control groups, in line with previous studies.[49,50] However, no significant differences in *Proteobacteria* and *Firmicutes* abundances were observed between the groups. *Deferribacterota*, although different, was present in very low numbers in both groups, with limited studies on its association with aging and hypertension.[51,52] The abundance of *Enterococcus* was significantly reduced in the feces of the NARDS patients. This genus activates host immune pathways and pathogen tolerance through its peptidoglycan composition and hydrolase activity.[53] Interestingly, the abundance of *Streptococcus* was increased in the feces of the NARDS_S group, whereas it was significantly reduced in the lower airway secretions of the NARDS patients. This aligns with Shen's findings in critically ill patients, suggesting it may be attributed to different *Streptococcus* species involved.[41] In summary, the gut microbiota of NARDS patients changes, but further exploration is needed to understand their impact on lung diseases.

Our study found significant changes in tryptophan metabolites in the lungs and plasma of NARDS patients. After absorption by the intestines, tryptophan can be metabolized by microbes into indoles and their derivatives, influencing the generation of kynurenine (KYN) and 3-hydroxyanthranilic acid (3-HAA) by regulating the key rate-limiting enzyme indoleamine 2,3-dioxygenase (IDO) in the kynurenine pathway.[23] Tryptophan metabolites play critical roles in many inflammatory diseases.[54,55] They can participate in respiratory system diseases by activating AhR, which is widely expressed and highly active in the lung barrier and immune system.[24,56] Previous studies have found that ICA exhibits anti-allergic and antimicrobial effects, while indole-3-acetic acid (IAA) may alleviate inflammation through IL-22, exerting protective effects in respiratory system diseases.[57–59] However, the role of ILA remains controversial, potentially exerting protective effects in conditions such as tumors and neurodegeneration, or being associated with chronic kidney disease, cisplatin-induced intestinal pathology, and colitis.[60–65] Additionally, the KYN/Trp ratio,

a biomarker reflecting underlying inflammation, is associated with poor cancer prognosis, increased risk of cardiovascular disease and mortality.[54,66–68] Consistent with our results, levels of ILA and KYN/Trp were significantly elevated in the lungs and plasma of NARDS neonates, while levels of ICA were significantly decreased in the lungs, and levels of 3-HK, IAA, ILA, IPA, IS, KYN, and Trp were significantly decreased in moderate to severe NARDS neonates' lungs. These decreased tryptophan metabolites may fail to exert effective anti-inflammatory and protective effects in NARDS neonates, potentially playing critical roles in disease progression. Therefore, tryptophan metabolites with significant changes in NARDS patients may be key compounds for treating the disease.

In this study, a significant correlation was observed between altered microbial communities and tryptophan metabolites in NARDS patients. Previous studies support our findings that AhR agonists are deficient in germ-free or dysbiotic mice, and *Lactobacillus* exert a wide range of anti-inflammatory and antioxidant activities through IAA and IPA.[54,69,70] Additionally, *Firmicutes* such as *Lactobacillus rossiae, L. johnsonii, and L. acidophilus* produce ICA, which is crucial for maintaining intestinal epithelial cells and defending against pathogens.[71,72] These findings underscore the close association between changes in microbiota and metabolites, which are closely related to disease progression. Therefore, it is attractive to consider the use of specific microbiota and metabolite variation in NARDS as biomarkers for disease identification and grading. Surprisingly, the variations in microbiota and metabolites in the lungs of NARDS patients exhibited discriminatory and grading significance, whereas the differential gut microbiota and plasma metabolites did not exhibit this capability. This suggests a closer association between changes in lung microbial communities and metabolites with disease progression. The lung microbiota and tryptophan metabolites, as biomarkers, are better suited for identifying NARDS and severity grading.

This study lacks a healthy control group. Due to limitations in the collection of respiratory secretion samples (typically only collected and tested in clinical respiratory disease cases), we chose NRDS or TTN patients as controls, but any disease may present changes in the microbial community. Additionally, there is a risk of contamination during the collection process of lower respiratory secretions and feces. All respiratory secretions were collected using sterile aspiration catheters inserted below the glottis. Fecal samples were collected from areas not in contact with the skin or diaper surface, thus minimizing the risk of contamination. In our study, there was no significant difference in antibiotic usage between the two groups, but due to the nature of the disease, there were differences in ventilation therapy between the groups. However, we attempted to collect cases as early as possible after birth to minimize the influence of confounding factors on the results. Due to the small sample size, we only preliminarily explored the changes in the overall microbial community and metabolites in the NARDS population. More patients are needed to further validate the results and to delve into the differences among different etiologies and risk factors.

Conclusion

This study, for the first time, integrated metagenomics and metabolomics and observed significant alterations in the lung-gut microbiota and lung-plasma tryptophan metabolites in NARDS patients, with a correlation between microbiota and metabolites. Additionally, the unique microbial compositions and tryptophan metabolites in the lungs demonstrated superior discriminatory and grading abilities for NARDS.

Data Sharing Statement

The raw data supporting the conclusions of this article will be made available by the corresponding author YS, without undue reservation.

Ethics Approval and Consent to Participate

The sample collection and analysis from human was approved by the ethics committee of the Children's Hospital of Chongqing Medical University.

Consent for Publication

All authors gave their consent for publication.

Acknowledgments

Dr Yang thanked Mr. Bo Lu for his help and support during the experiment.

Author Contributions

All authors have contributed significantly to the reported work, including conception, study design, execution, data acquisition, analysis, and interpretation. Additionally, all authors have reached an agreement on the journal to which the article has been submitted and accept responsibility for all aspects of the work.

Funding

This study was supported by National Key Research and Development Program of China (No.2022YFC2704802), the National Natural Science Foundation of China (No. 82001602), Special Funding for Postdoctoral Research Projects of Chongqing (No. 2022CQBSHTB3085), and China Postdoctoral Science Foundation (No.2023MD744152).

Disclosure

The authors report no conflicts of interest in this work.

References

1. Chi M, Mei YB, Feng ZC. A review on neonatal acute respiratory distress syndrome. *Zhongguo Dang Dai Er Ke Za Zhi*. 2018;20(9):724–728. doi:10.7499/j.issn.1008-8830.2018.09.006
2. De Luca D, Tingay DG, van Kaam AH, et al. Epidemiology of neonatal acute respiratory distress syndrome: prospective, multicenter, international cohort study. *Pediatr Crit Care Med*. 2022;23(7):524–534. doi:10.1097/PCC.0000000000002961
3. Rooks MG, Garrett WS. Gut microbiota, metabolites and host immunity. *Nat Rev Immunol*. 2016;16(6):341–352. doi:10.1038/nri.2016.42
4. Cryan JF, O'Riordan KJ, Cowan C, et al. The microbiota-gut-brain axis. *Physiol Rev*. 2019;99(4):1877–2013. doi:10.1152/physrev.00018.2018
5. Agus A, Planchais J, Sokol H. Gut microbiota regulation of tryptophan metabolism in health and disease. *Cell Host Microbe*. 2018;23(6):716–724. doi:10.1016/j.chom.2018.05.003
6. Budden KF, Gellatly SL, Wood DL, et al. Emerging pathogenic links between microbiota and the gut-lung axis. *Nat Rev Microbiol*. 2017;15(1):55–63. doi:10.1038/nrmicro.2016.142
7. Wypych TP, Wickramasinghe LC, Marsland BJ. The influence of the microbiome on respiratory health. *Nat Immunol*. 2019;20(10):1279–1290. doi:10.1038/s41590-019-0451-9
8. Natalini JG, Singh S, Segal LN. The dynamic lung microbiome in health and disease. *Nat Rev Microbiol*. 2023;21(4):222–235. doi:10.1038/s41579-022-00821-x
9. Budden KF, Shukla SD, Rehman SF, et al. Functional effects of the microbiota in chronic respiratory disease. *Lancet Respir Med*. 2019;7(10):907–920. doi:10.1016/S2213-2600(18)30510-1
10. Freestone PP, Hirst RA, Sandrini SM, et al. Pseudomonas aeruginosa-catecholamine inotrope interactions: a contributory factor in the development of ventilator-associated pneumonia? *Chest*. 2012;142(5):1200–1210. doi:10.1378/chest.11-2614
11. Zhang P, Liu B, Zheng W, et al. Pulmonary microbial composition in sepsis-induced acute respiratory distress syndrome. *Front Mol Biosci*. 2022;9:862570. doi:10.3389/fmolb.2022.862570
12. Huffnagle GB, Dickson RP, Lukacs NW. The respiratory tract microbiome and lung inflammation: a two-way street. *Mucosal Immunol*. 2017;10(2):299–306. doi:10.1038/mi.2016.108
13. He Y, Wen Q, Yao F, et al. Gut-lung axis: the microbial contributions and clinical implications. *Crit Rev Microbiol*. 2017;43(1):81–95. doi:10.1080/1040841X.2016.1176988
14. Pattaroni C, Watzenboeck ML, Schneidegger S, et al. Early-life formation of the microbial and immunological environment of the human airways. *Cell Host Microbe*. 2018;24(6):857–865. doi:10.1016/j.chom.2018.10.019
15. de Vos WM, Tilg H, Van Hul M, et al. Gut microbiome and health: mechanistic insights. *Gut*. 2022;71(5):1020–1032. doi:10.1136/gutjnl-2021-326789
16. Ashique S, De Rubis G, Sirohi E, et al. Short Chain Fatty Acids: fundamental mediators of the gut-lung axis and their involvement in pulmonary diseases. *Chem Biol Interact*. 2022;368:110231. doi:10.1016/j.cbi.2022.110231
17. Pabst O, Hornef MW, Schaap FG, et al. Gut-liver axis: barriers and functional circuits. *Nat Rev Gastroenterol Hepatol*. 2023;20(7):447–461. doi:10.1038/s41575-023-00771-6
18. Liu M, Nieuwdorp M, de Vos WM, et al. Microbial tryptophan metabolism tunes host immunity, metabolism, and extraintestinal disorders. *Metabolites*. 2022;12(9):834. doi:10.3390/metabo12090834
19. Rothhammer V, Mascanfroni ID, Bunse L, et al. Type I interferons and microbial metabolites of tryptophan modulate astrocyte activity and central nervous system inflammation via the aryl hydrocarbon receptor. *Nat Med*. 2016;22(6):586–597. doi:10.1038/nm.4106
20. Gao K, Mu CL, Farzi A, et al. Tryptophan metabolism: a link between the gut microbiota and brain. *Adv Nutr*. 2020;11(3):709–723. doi:10.1093/advances/nmz127
21. Qi Q, Li J, Yu B, et al. Host and gut microbial tryptophan metabolism and type 2 diabetes: an integrative analysis of host genetics, diet, gut microbiome and circulating metabolites in cohort studies. *Gut*. 2022;71(6):1095–1105. doi:10.1136/gutjnl-2021-324053
22. Liu Y, Pei Z, Pan T, et al. Indole metabolites and colorectal cancer: gut microbial tryptophan metabolism, host gut microbiome biomarkers, and potential intervention mechanisms. *Microbiol Res*. 2023;272:127392. doi:10.1016/j.micres.2023.127392

23. Su X, Gao Y, Yang R. Gut microbiota-derived tryptophan metabolites maintain gut and systemic homeostasis. *Cells*. 2022;11(15):2296. doi:10.3390/cells11152296
24. Major J, Crotta S, Finsterbusch K, et al. Endothelial AHR activity prevents lung barrier disruption in viral infection. *Nature*. 2023;621(7980):813–820. doi:10.1038/s41586-023-06287-y
25. De Luca D, van Kaam AH, Tingay DG, et al. The Montreux definition of neonatal ARDS: biological and clinical background behind the description of a new entity. *Lancet Respir Med*. 2017;5(8):657–666. doi:10.1016/S2213-2600(17)30214-X
26. Chen L, Li J, Shi Y. Clinical characteristics and outcomes in neonates with perinatal acute respiratory distress syndrome in China: a national, multicentre, cross-sectional study. *EClinicalMedicine*. 2023;55:101739. doi:10.1016/j.eclinm.2022.101739
27. Bruschettini M, Hassan KO, Romantsik O, et al. Interventions for the management of transient tachypnoea of the newborn - an overview of systematic reviews. *Cochrane Database Syst Rev*. 2022;2:D13563.
28. Enav H, Backhed F, Ley RE. The developing infant gut microbiome: a strain-level view. *Cell Host Microbe*. 2022;30(5):627–638. doi:10.1016/j.chom.2022.04.009
29. Sakonidou S, Dhaliwal J. The management of neonatal respiratory distress syndrome in preterm infants (European Consensus Guidelines--2013 update). *Arch Dis Child Educ Pract Ed*. 2015;100(5):257–259. doi:10.1136/archdischild-2014-306642
30. Alhassen Z, Vali P, Guglani L, et al. Recent advances in pathophysiology and management of transient tachypnea of newborn. *J Perinatol*. 2021;41(1):6–16. doi:10.1038/s41372-020-0757-3
31. Hooper LV, Macpherson AJ. Immune adaptations that maintain homeostasis with the intestinal microbiota. *Nat Rev Immunol*. 2010;10(3):159–169. doi:10.1038/nri2710
32. Cani PD. Human gut microbiome: hopes, threats and promises. *Gut*. 2018;67(9):1716–1725. doi:10.1136/gutjnl-2018-316723
33. Dickson RP, Erb-Downward JR, Huffnagle GB. Homeostasis and its disruption in the lung microbiome. *Am J Physiol Lung Cell Mol Physiol*. 2015;309(10):L1047–L1055. doi:10.1152/ajplung.00279.2015
34. Huang YJ, Nariya S, Harris JM, et al. The airway microbiome in patients with severe asthma: associations with disease features and severity. *J Allergy Clin Immunol*. 2015;136(4):874–884. doi:10.1016/j.jaci.2015.05.044
35. Wang J, Chai J, Zhang L, et al. Microbiota associations with inflammatory pathways in asthma. *Clin Exp Allergy*. 2022;52(5):697–705. doi:10.1111/cea.14089
36. Bernasconi E, Pattaroni C, Koutsokera A, et al. Airway microbiota determines innate cell inflammatory or tissue remodeling profiles in lung transplantation. *Am J Respir Crit Care Med*. 2016;194(10):1252–1263. doi:10.1164/rccm.201512-2424OC
37. Dicker AJ, Huang J, Lonergan M, et al. The sputum microbiome, airway inflammation, and mortality in chronic obstructive pulmonary disease. *J Allergy Clin Immunol*. 2021;147(1):158–167. doi:10.1016/j.jaci.2020.02.040
38. Siwicka-Gieroba D, Czarko-Wicha K. Lung microbiome - A modern knowledge. *Cent Eur J Immunol*. 2020;45(3):342–345. doi:10.5114/ceji.2020.101266
39. Puccetti M, Pariano M, Costantini C, et al. Pharmaceutically active microbial AhR agonists as innovative biodrugs in inflammation. *Pharmaceuticals*. 2022;15(3):336. doi:10.3390/ph15030336
40. Ahlawat S, Asha, Sharma KK. Gut-organ axis: a microbial outreach and networking. *Lett Appl Microbiol*. 2021;72(6):636–668. doi:10.1111/lam.13333
41. Shen Y, Yu F, Zhang D, et al. Dynamic alterations in the respiratory tract microbiota of patients with COVID-19 and its association with microbiota in the gut. *Adv Sci*. 2022;9(27):e2200956. doi:10.1002/advs.202200956
42. Rigauts C, Aizawa J, Taylor SL, et al. Rothia mucilaginosa is an anti-inflammatory bacterium in the respiratory tract of patients with chronic lung disease. *Eur Respir J*. 2022;59(5):2101293. doi:10.1183/13993003.01293-2021
43. Kolling Y, Salva S, Villena J, et al. Non-viable immunobiotic Lactobacillus rhamnosus CRL1505 and its peptidoglycan improve systemic and respiratory innate immune response during recovery of immunocompromised-malnourished mice. *Int Immunopharmacol*. 2015;25(2):474–484. doi:10.1016/j.intimp.2015.02.006
44. Ksonzekova P, Bystricky P, Vlckova S, et al. Exopolysaccharides of Lactobacillus reuteri: their influence on adherence of E. coli to epithelial cells and inflammatory response. *Carbohydr Polym*. 2016;141:10–19. doi:10.1016/j.carbpol.2015.12.037
45. Percopo CM, Dyer KD, Garcia-Crespo KE, et al. B cells are not essential for lactobacillus-mediated protection against lethal pneumovirus infection. *J Immunol*. 2014;192(11):5265–5272. doi:10.4049/jimmunol.1400087
46. Forsythe P, Inman MD, Bienenstock J. Oral treatment with live lactobacillus reuteri inhibits the allergic airway response in mice. *Am J Respir Crit Care Med*. 2007;175(6):561–569. doi:10.1164/rccm.200606-821OC
47. Carvalho JL, Miranda M, Fialho AK, et al. Oral feeding with probiotic Lactobacillus rhamnosus attenuates cigarette smoke-induced COPD in C57Bl/6 mice: relevance to inflammatory markers in human bronchial epithelial cells. *PLoS One*. 2020;15(4):e225560. doi:10.1371/journal.pone.0225560
48. Bidossi A, De Grandi R, Toscano M, et al. Probiotics Streptococcus salivarius 24SMB and Streptococcus oralis 89a interfere with biofilm formation of pathogens of the upper respiratory tract. *BMC Infect Dis*. 2018;18(1):653. doi:10.1186/s12879-018-3576-9
49. Galazzo G, van Best N, Bervoets L, et al. Development of the microbiota and associations with birth mode, diet, and atopic disorders in a longitudinal analysis of stool samples, collected from infancy through early childhood. *Gastroenterology*. 2020;158(6):1584–1596. doi:10.1053/j.gastro.2020.01.024
50. Backhed F, Roswall J, Peng Y, et al. Dynamics and stabilization of the human gut microbiome during the first year of life. *Cell Host Microbe*. 2015;17(5):690–703. doi:10.1016/j.chom.2015.04.004
51. Ratto D, Roda E, Romeo M, et al. The many ages of microbiome-gut-brain axis. *Nutrients*. 2022;15(1):14. doi:10.3390/nu15010014
52. Shi H, Nelson JW, Phillips S, et al. Alterations of the gut microbial community structure and function with aging in the spontaneously hypertensive stroke prone rat. *Sci Rep*. 2022;12(1):8534. doi:10.1038/s41598-022-12578-7
53. Kim B, Wang YC, Hespen CW, et al. Enterococcus faecium secreted antigen A generates muropeptides to enhance host immunity and limit bacterial pathogenesis. *Elife*. 2019;8:e45343.
54. Lamas B, Richard ML, Leducq V, et al. CARD9 impacts colitis by altering gut microbiota metabolism of tryptophan into aryl hydrocarbon receptor ligands. *Nat Med*. 2016;22(6):598–605. doi:10.1038/nm.4102

55. Lavelle A, Sokol H. Gut microbiota-derived metabolites as key actors in inflammatory bowel disease. *Nat Rev Gastroenterol Hepatol*. 2020;17(4):223–237. doi:10.1038/s41575-019-0258-z
56. Lamas B, Natividad JM, Sokol H. Aryl hydrocarbon receptor and intestinal immunity. *Mucosal Immunol*. 2018;11(4):1024–1038. doi:10.1038/s41385-018-0019-2
57. Romani L, Zelante T, De Luca A, et al. Microbiota control of a tryptophan-AhR pathway in disease tolerance to fungi. *Eur J Immunol*. 2014;44(11):3192–3200. doi:10.1002/eji.201344406
58. Puccetti M, Paolicelli G, Oikonomou V, et al. Towards targeting the aryl hydrocarbon receptor in cystic fibrosis. *Mediators Inflamm*. 2018;2018:1601486. doi:10.1155/2018/1601486
59. Yan Z, Chen B, Yang Y, et al. Multi-omics analyses of airway host-microbe interactions in chronic obstructive pulmonary disease identify potential therapeutic interventions. *Nat Microbiol*. 2022;7(9):1361–1375. doi:10.1038/s41564-022-01196-8
60. Ehrlich AM, Pacheco AR, Henrick BM, et al. Indole-3-lactic acid associated with Bifidobacterium-dominated microbiota significantly decreases inflammation in intestinal epithelial cells. *BMC Microbiol*. 2020;20(1):357. doi:10.1186/s12866-020-02023-y
61. Han JX, Tao ZH, Wang JL, et al. Microbiota-derived tryptophan catabolites mediate the chemopreventive effects of statins on colorectal cancer. *Nat Microbiol*. 2023;8(5):919–933. doi:10.1038/s41564-023-01363-5
62. Yin J, Zhang Y, Liu X, et al. Gut microbiota-derived indole derivatives alleviate neurodegeneration in aging through activating GPR30/AMPK/SIRT1 pathway. *Mol Nutr Food Res*. 2023;67(9):e2200739. doi:10.1002/mnfr.202200739
63. Miao H, Wang YN, Yu XY, et al. Lactobacillus species ameliorate membranous nephropathy through inhibiting the aryl hydrocarbon receptor pathway via tryptophan-produced indole metabolites. *Br J Pharmacol*. 2023;181(1):162–179. doi:10.1111/bph.16219
64. Zou YT, Zhou J, Wu CY, et al. Protective effects of Poria cocos and its components against cisplatin-induced intestinal injury. *J Ethnopharmacol*. 2021;269:113722. doi:10.1016/j.jep.2020.113722
65. Fan Q, Guan X, Hou Y, et al. Paeoniflorin modulates gut microbial production of indole-3-lactate and epithelial autophagy to alleviate colitis in mice. *Phytomedicine*. 2020;79:153345. doi:10.1016/j.phymed.2020.153345
66. Sulo G, Vollset SE, Nygard O, et al. Neopterin and kynurenine-tryptophan ratio as predictors of coronary events in older adults, the Hordaland Health Study. *Int J Cardiol*. 2013;168(2):1435–1440. doi:10.1016/j.ijcard.2012.12.090
67. Zuo H, Ueland PM, Ulvik A, et al. Plasma biomarkers of inflammation, the kynurenine pathway, and risks of all-cause, cancer, and cardiovascular disease mortality: the hordaland health study. *Am J Epidemiol*. 2016;183(4):249–258. doi:10.1093/aje/kwv242
68. Sorgdrager F, Naude P, Kema IP, et al. Tryptophan metabolism in inflammaging: from biomarker to therapeutic target. *Front Immunol*. 2019;10:2565. doi:10.3389/fimmu.2019.02565
69. Dang G, Wen X, Zhong R, et al. Pectin modulates intestinal immunity in a pig model via regulating the gut microbiota-derived tryptophan metabolite-AhR-IL22 pathway. *J Anim Sci Biotechnol*. 2023;14(1):38. doi:10.1186/s40104-023-00838-z
70. Venkatesh M, Mukherjee S, Wang H, et al. Symbiotic bacterial metabolites regulate gastrointestinal barrier function via the xenobiotic sensor PXR and Toll-like receptor 4. *Immunity*. 2014;41(2):296–310. doi:10.1016/j.immuni.2014.06.014
71. Cervantes-Barragan L, Chai JN, Tianero MD, et al. Lactobacillus reuteri induces gut intraepithelial CD4(+)CD8alphaalpha(+) T cells. *Science*. 2017;357(6353):806–810. doi:10.1126/science.aah5825
72. Gutierrez-Vazquez C, Quintana FJ. Regulation of the immune response by the aryl hydrocarbon receptor. *Immunity*. 2018;48(1):19–33. doi:10.1016/j.immuni.2017.12.012